Appendix: Crustal controls on apparent mantle pyroxenite signals

Matthew L. M. Gleeson[1], **Sally A. Gibson**[1]

[1]Department of Earth Sciences, University of Cambridge,
Downing Street, Cambridge, UK, CB2 3EQ

mlmg3@cam.ac.uk

1. Analytical Methodology

Approximately 65 olivine phenocrysts from the eastern Galápagos were analysed using a Cameca SX100 EPMA in the Department of Earth Sciences, University of Cambridge. Run conditions of 15 keV and 20 nA were used for Si, Fe and Mg. The beam current was increased to 100 nA for Ni, Mn, Ca, and Al in order to increase precision. A 5 μm spot was used for all analyses. A combination of mineral and metal standards were used for calibration at the start of each analytical session (Fayalite - Fe; Diopside - Ca, Si; St. Johns Olivine - Mg; Jadeite - Na; Corundum - Al; Mn and Ni metal for Mn and Ni respectively). Precision and accuracy were monitored using a San Carlos Olivine secondary standard at regular intervals. Recovery for Fe, Si and Mg is consistently between 98.5 and 100% for all analyses of secondary standards. Recovery of Mn and Ni is also excellent, consistently between 99 and 103%. Ca displays slightly lower recovery values around 95% for most analytical sessions. Two-sigma precision is better than 3% for Fe, and consistently better than 1.5% for Mg and Si. Ni, Ca and Mn display 2σ precision of $<$4%, $<$15% and $<$8% respectively.

2. Heterogeneity in the Galápagos mantle plume

Compositional heterogeneity in recently erupted basalts from across the Galápagos Archipelago result from the melting of at least 4 isotopically distinct mantle domains (Geist et al., 1988; Harpp and White, 2001; Hoernle et al., 2000; White et al., 1993). Three isotopically enriched domains (which are each most prevalent in distinct regions of the archipelago) form a horseshoe-shaped pattern around the isotopically depleted eastern domain (Harpp and White, 2001; White et al., 1993). The isotopically enriched components are characterised by high $^3He/^4He$ ratios in the western archipelago (central isotopic domain), extremely radiogenic Pb-isotope compositions in the southern archipelago (southern domain), and a northern isotopic domain that displays moderately radiogenic Sr and Pb isotope ratios and characteristicly high ratios of $^{208}Pb/^{206}Pb$ and $^{207}Pb/^{206}Pb$.

These isotopically enriched domains in the Galapagos mantle surround the isotopically depleted eastern domain (Islas Santiago, Santa Cruz, Genovesa etc.; Fig S.1). Basalts erupted in this region tend to be tholeiitic, and display Sr and Pb isotope signatures similar to many N-MORBs observed globally (Harpp and White, 2001). It is these basalts that are of particular interest for this study as recent work into the composition of olivine phenocrysts from these islands indicated that there must be a large contribution from a pyroxenitic component in the mantle source (Vidito et al., 2013), contradicting major-element and isotopic evidence for a dominantly peridotitic source (Gibson et al., 2012).

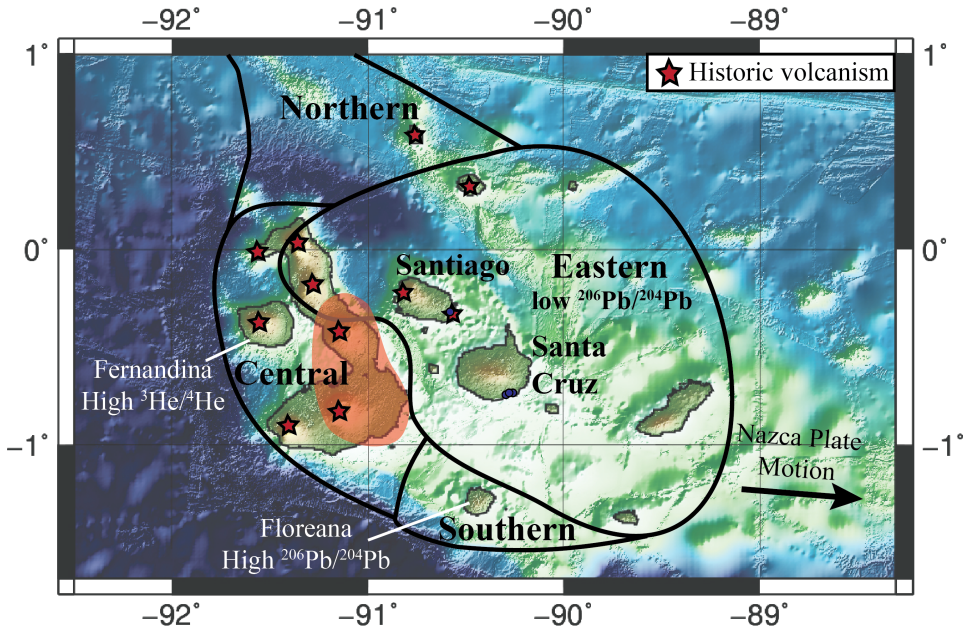

Fig S.1: *Map of the Galapagos archipelago showing the location of Santiago and Santa Cruz with respect to the different isotopic domains from Hoernle et al. (2000). Location of the plume stem is taken from Villagomez et al. (2014).*

For the purposes of this study we analyse the composition of olivine phenocrysts in 3 samples from SE Santa Cruz (Longitude: 90.3219^{o}W; Latitude: 0.749^{o}N), a region that displays relatively unradiogenic Sr and Pb isotope compositions (White et al, 1993). This is complemented by new analyses of olivine compositions from eastern Santiago basalts (sample 07DSG75; Longitude: 90.3417^{o}W; Latitude: 0.1761^{o}N), as well as olivine data collected by Gibson et al. (2016).

3. Major-element systematics of low-K tholeiitic basalts from the eastern Galápagos

We have shown that the olivine chemistry from eastern Galápagos tholeiite basalts is consistent with a peridotite source, but it is informative to consider whether this interpretation is consistent with other available evidence. As previously stated, eastern Galápagos tholeiitic basalts display radiogenic isotope ratios similar to those observed in MORBs (Gibson et al., 2012), which appears to indicate a similar mantle source. Additionally, major element concentrations in high MgO basalts (>9wt%) have been shown to be sensitive to the source lithology from which they formed, and have been used in many previous studies to infer lithological heterogeneity in the mantle source region of OIBs (Hauri, 1996; Dasgupta et al., 2009; Lambart et al., 2009; Shorttle and Maclennan, 2011; Shorttle et al., 2014). We therefore investigate whether the major element chemistry of high-MgO tholeiitic basalts from Isla Santiago are consistent with a peridotite source by comparing published whole-rock compositions to the results of melting experiments on peridotite starting materials. Isla Santiago was chosen in this case due to the presence of a large, well characterised dataset for high MgO basalts (Gibson et al., 2012).

Comparison of tholeiitic basalts from Santiago with melting experiments on peridotite starting materials is shown in Fig. S2. Olivine fractionation curves for melting

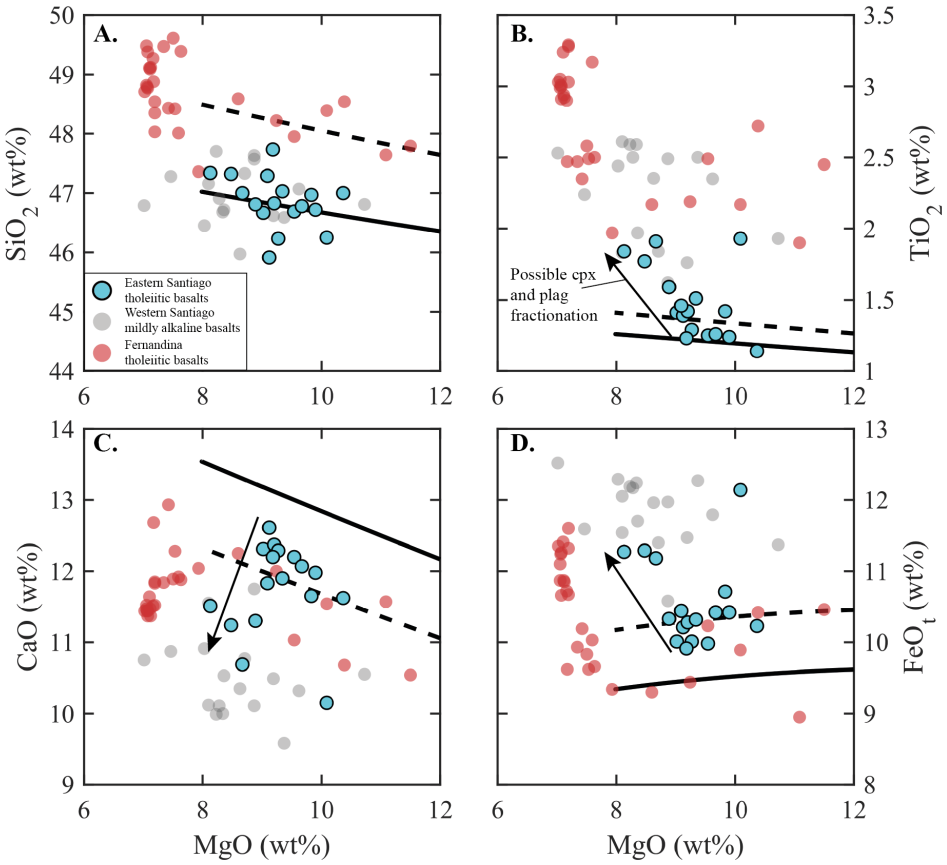

Fig S.2: *Major-element variation seen in tholeiitic basalts from eastern Santiago. Also shown are the composition of isotopically-enriched, mildly-alkaline basalts from western Santiago and tholeiitic basalts from Isla Fernandina. Black lines show the olivine subtraction curves for two melt experiments on lherzolitic starting materials (KLB-1, 3 GPa, 1500° - solid; Hirose, 1993; HK66, 2 GPa, 1425° - dashed; Hirose and Kushiro, 1993). Data from Isla Santiago is taken from Gibson et al., (2012) and data from Fernandina is taken from Geist et al. (2006).*

experiments at 3 GPa and 1500°C on peridotite KLB-1 (solid line) and at 2 GPa and 1425°C on composition HK66 are shown (experimental data from Hirose and Kushiro, 1993). It can be clearly seen from Fig. S.2 that the major-element systematics of these basalts are reasonably well approximated by melting of a peridotite source and are in agreement with our interpretations of olivine chemistry in these basalts.

4. Petrographic description

All Galápagos samples under analysis are olivine and plagioclase phyric with rare clinopyroxene. Some samples possess a glassy, nearly microlite-free matrix (e.g. 07DSG75) whereas others have a coarsely-crystalline matrix (crystals 100μm in length) in which the groundmass and smaller phenocrysts are nearly indistinguishable petrographically. Plagioclase and olivine commonly occur in crystal clots several mm in size. In all samples oscillatory zoning is observed in the plagioclase phenocrysts (both individual crystals and in crystal clots), however, in sample 07DSG75 this zoning is much less common. Plagioclase crystals are generally euhedral and have a high aspect ratio.

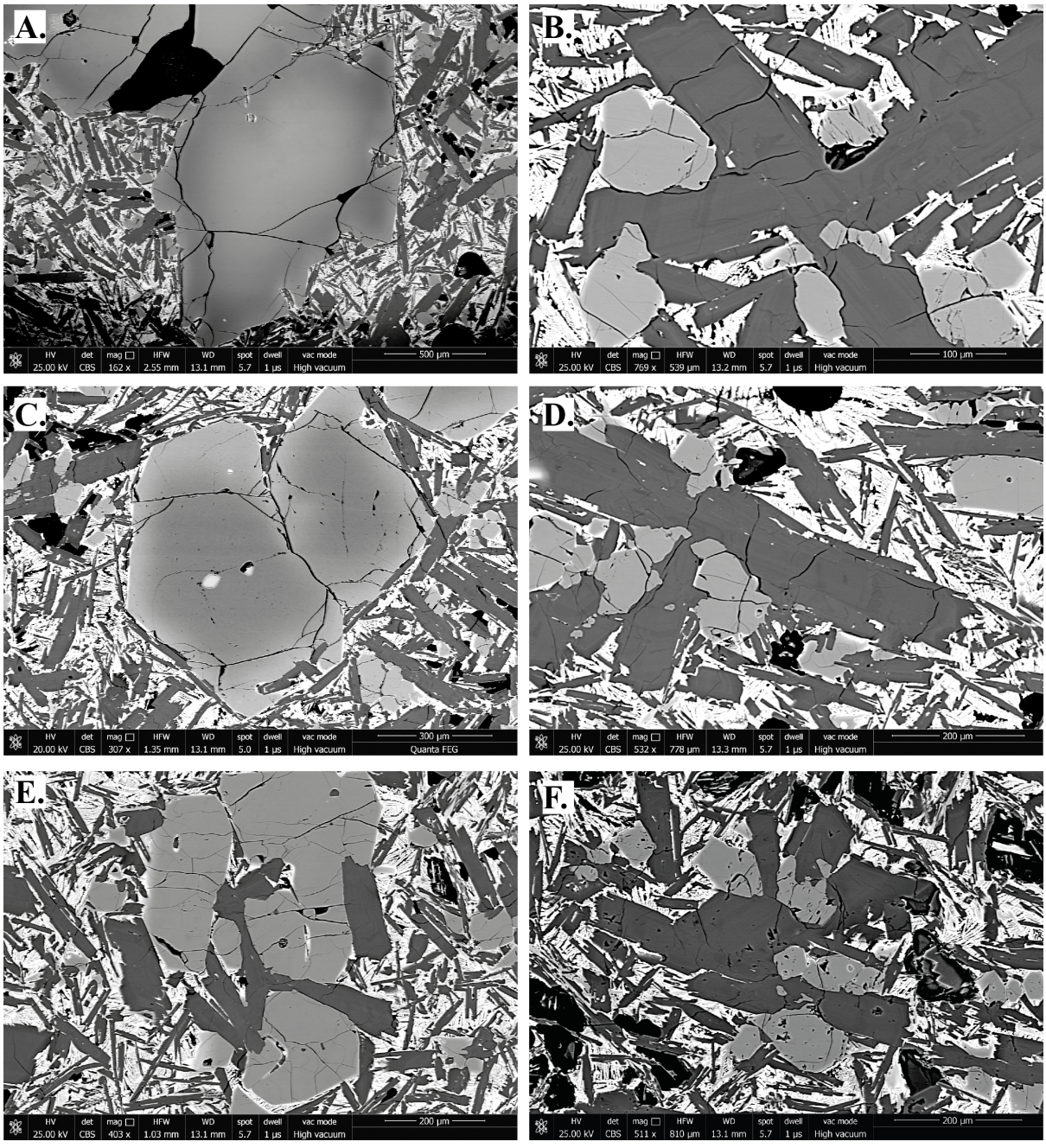

Fig S.3: *Back-Scatter Electron (BSE) images of olvines (**A. C. E.**) and plagioclase (**B. D. F.**) phenocrysts and crystal clots in Santa Cruz sample 07DSG83. This sample displays many of the petrographic features seen in nearly all of the Santa Cruz and Santiago basalts under study. Olivine 3 from samples 07DSG83 is shown in **A.**. Oscillatory zoning is seen in all plagioclase crystals, but olivine crystals are generally unzoned, or possess a narrow normally zoned rim. Only a handful of larger olivine crystals preserve reversely-zoned cores.*

Olivine crystals in most samples occur as unzoned (usually associated with olivine-plagioclase crystal clots) and normally-zoned crystals where the zoned rims can be up to 200μm wide. Additionally, in several samples many larger olivines show reverse-zoning profiles up to 2mm in length as well as an outer, normally-zoned rim (Fig. S.3). Olivine crystals are generally euhedral to subhedral although dissolution textures are seen in some samples. The presence of complex zoning in both olivine and plagioclase indicates a complex magmatic history involving the interaction of several chemically distinct magmas.

5. Influence of crystallsation pressure - clinopyroxene phase stability

Hole (2018) recently investigated the role of pressure on the concentration of Ni and Ca in olivines crystallising in continental flood basalts. Their results showed that high-pressure crystallisation (>1.6 GPa) could explain the high Ni and low Ca contents of olivine phenocrysts from the British Palaeogene Igneous Province, due to the influence of pressure on clinopyroxene stability.

At high pressure, the clinopyroxene phase field expands at the expense of olivine and plagioclase (O'Hara, 1968). Consequently, clinopyroxene becomes a crystallising phase earlier during fractional crystallisation of high-MgO basalts at high pressures. As Ni partitions less strongly into clinopyroxene than olivine (Sobolev et al. 2007), co-crystallisation of olivine and clinopyroxene causes a reduction in the rate that the Ni content of the melt decreases relative to the Mg# of the melt. Therefore, high-pressure crystallisation results in olivine compositions that have high Ni contents at a set Fo content. Additionally, high-pressure crystallisation of clinopyroxene results in a significant decrease in the Ca content of the melt and subsequent olivine phenocrysts.

6. Influence of pressure and temperature on the partitioning of Ni

Recent experimental studies have indicated that the partitioning of Ni between olivine and silicate melt may be highly sensitive to the conditions of mantle melting and the composition of the resulting melts (Matzen et al., 2013; 2017). These authors suggest that the increased pressure of melting beneath ocean islands, and the higher mantle potential temperatures in these regions, results in higher average temperatures of melt formation compared to mid-ocean ridges. At higher temperature, Ni partitions less strongly into olivine, so the resulting melts from a peridotite source should have higher Ni contents than melts formed at lower temperatures (Matzen et al., 2013; 2017).

In order to estimate the Ni concentration of primary melts that erupted in the eastern Galápagos, Réunion and the Canary Islands, we used the Melt-PX model of Lambart et al. (2016) to estimate the temperature of the mantle at the top of the melt column for lherzolitic mantle at a mantle potential temperature of 1400°C that is undergoing adiabatic decompression melting. The Ni partitioning between olivine and silicate melt was then estimated using the method of Matzen et al. (2017). The temperature was taken from Melt-PX at ~2-2.5 GPa and the MgO content of the melt was set at 16.7 wt% for Galápagos and 14.5 wt% for Réunion and the Canaries. The MgO content was chosen based on the MgO content of Santiago sample 07DSG72 fractionation corrected to be in equilibrium with mantle peridotite and Tenerife sample TF2 (Gurenko et al., 2006). Assuming that primary magmas formed from mantle with olivines containing ~2960 ppm Ni, the Ni content of the coexisting melt is calculated to be 505-515 ppm using the model of Matzen et al. (2017). Although simplistic, this modelling demonstrates that melts of a

peridotitic source beneath eastern Santiago can result in elevated Ni contents in primary mantle melts.

7. Diffusion model

Our diffusion model simulates the re-equilibration of a distribution of high-Fo olivines, formed during the first stages of crystallisation of a peridotite-derived melt, with a magma formed via mixing and homogenisation of a primitive mantle melt and a more evolved basaltic melt. To do this, a Guassian distribution of olivine compositions is generated. This is based on the work of Thompson and Maclennan (2013) who showed that olivines in a cumulate mush pile will tend to diffusively re-equilibrate towards the mean, resulting in a Guassian distribution. The Ni concentration of the starting olivines were then calculated using the fractional crystallisation trajectories generated by Petrolog.

The olivine compositions in equilibrium with the hybrid melt is set at Fo = 86.9 and Ni = 2300 ppm. This composition is equivalent to that predicted following the second period of magma recharge in the models shown in Figure 1 of the main text.

The olivines were allowed to diffusively re-equilibrate with this melt for 1, 10, and 30 years. Diffusion coefficients from Chakraborty (2010) were used. Numerical solutions to the diffusion equation presented in Girona and Costa (2013) were used to calculate diffusion profiles (Eq. 1). Time intervals of 1 hour were used, and modelled concentrations were calculated every 10 μm throughout the hypothetical olivine phenocryst.

$$C_i^{k,j+1} = C_i^{k,j} + \frac{\Delta t}{(\Delta x)^2}\left((C_i^{k+1,j} - C_i^{k,j})\frac{dD_i}{dX_{Fo}}\mid_{k,j,X_{Fo}} + (C_i^{k+1,j} - 2C_i^{k,j} + C_i^{k-1,j})D_i \mid_{k,j,X_{Fo}}\right) \quad (1)$$

Following diffusion, each olivine was randomly sampled for its chemical composition. This was achieved by generating a random plane in 3-dimensional space to 'section' the hypothetical olivines, and taking 'apparent core compositions' of the plane (i.e. the point closest to the true centre of the hypothetical crystal; the outer 100 μm of each olivine was excluded from possible analysis).

Full 3D anisotropic diffusion models (such as those applied by Shea et al., 2015 and Lynn et al., 2017) are computationally expensive and modelling diffusion in a single olivine for 1-2 years may take several days. By making a couple of simplifications to our model we are able to model diffusional re-equilibration for 200 olivines in approximately 3 hours. To do this, we assumed isotropic diffusion in spherical olivine crystals. For most models shown, isotropic diffusion using the diffusivity along the c-axis of an olivine was assumed. Our models were run at an oxygen fugacity of QFM, pressure was set at 500 MPa, and temperature was set at 1250°C.

8. Influence of magma mixing and recharge on olivine compositions from MORB lavas

As our model of magma recharge and mixing successfully reproduces the olivine chemistry of many OIBs it is important to consider whether this process influences the olivine chemistry of MORBs. Several studies have suggested that the geochemical signatures of many MORBs (especially at fast and intermediate spreading centres) are best explained

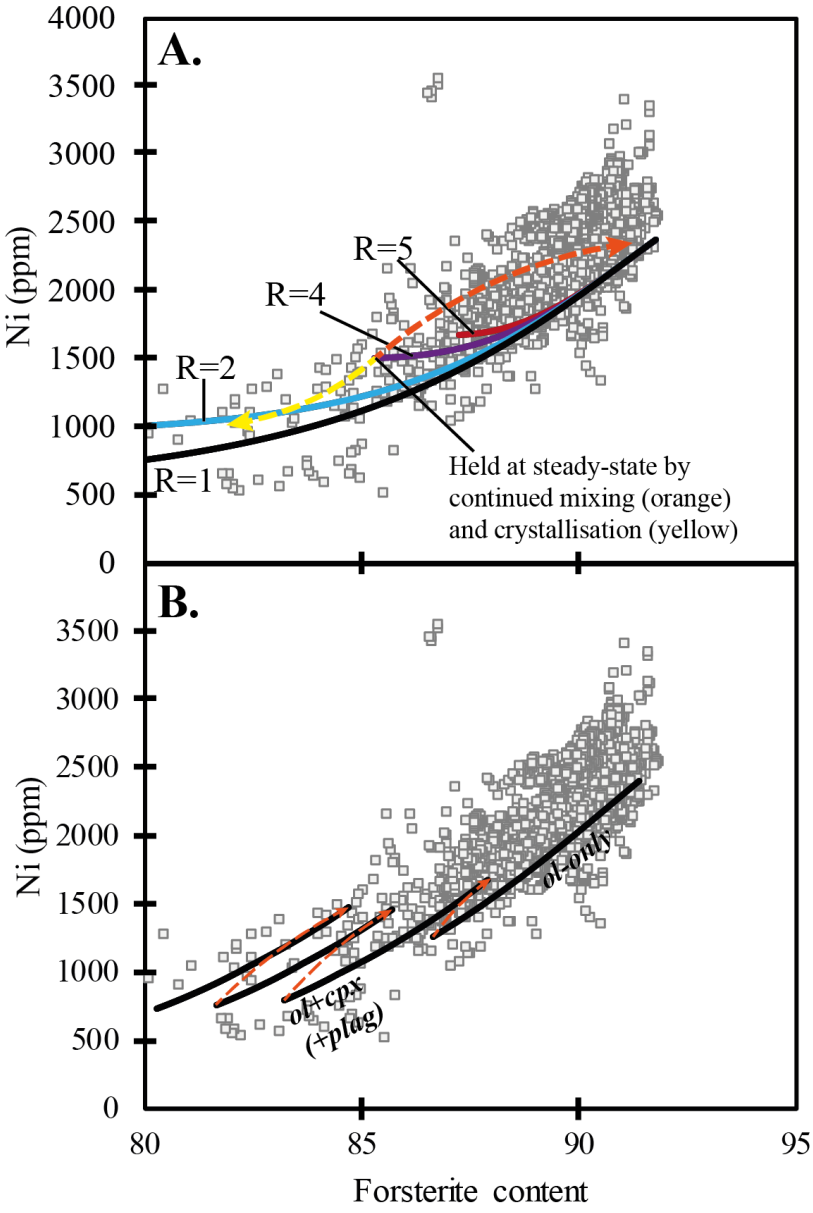

Fig S.4: *Olivine compositions from MORB lavas (data from Sobolev et al., 2007) compared to results of RTX magma chamber models.* ***A.*** *The R values of each curve represent the ratio between the mass of mafic magma introduced into the system at each step and the mass of crystallising products formed at each step.* ***B.*** *Results of crystallisation model where 16% crystallisation and 4% eruption is allowed to occur between each period of recharge.*

by open-system processes in a Replenished-Tapped-Crystallising (RTX) magma chamber (O'Neil and Jenner, 2012; Coogan and O'Hara, 2015). According to these studies, the system is continuously replenished by new mafic magma, tapped by eruption, and crystallises solid phases (olivine, clinopyroxene, plagioclase), resulting in the observed over-enrichments in incompatible trace elements (O'Neil and Jenner, 2012).

To investigate the influence of continuous magma recharge in a RTX magma chamber on olivine compositions we adjust our previous model to incorporate continuous recharge of mafic magma into an evolving magmatic system in two separate ways. First, we model continuous magma replenishment at every crystallsation interval (i.e. continuous replenishment defined by the ratio of mass replenished to mass crystallised). Secondly, we assume that for each 'cycle', approximately 16% crystallisation occurs, 4% of the initial magma is erupted and magma replenishment keeps the system at a steady state. These parameters where chosen to be consistent with the recent study of MORB chemistry by Coogan and O'Hara (2015). These models are achieved by using Santiago sample 07DSG72, fractionation corrected to be in equilibrium with mantle peridotite, as a starting composition. We then calculate the Ni contents of olivine phenocrysts that are predicted to fractionate (using the same parameters as described in the main text).

For the first model, magma replenishment occurs at every crystallisation interval in the model. The results are shown in Fig. S.4 and clearly show that continuous replenishment of a crystallising and tapped magma chamber results in a slight enrichment of Ni in olivine. This is most prevalent at moderately-high replenishment rates (ratio of mass of replenishment to mass crystallised of approximately 4) where the system reaches a steady-state crystallising olivine with a composition of approximately Fo 85 and 1500 ppm Ni. In the second model (Fig. S.4b) replenishment occurs after 16% crystallisation occurs and 4% of the initial magma is erupted. Replenishment allows the system to maintain a constant mass and results in a slight enrichment in the Ni content of the model olivines. These model olivines accurately match the composition of MORB-derived olivines which have Fo contents of 85 or less.

Therefore, it can be observed that during differentiation in a RTX magma chamber the extent of Ni enrichment is far smaller than that observed in a system where magma recharge occurs infrequently and represents a significant mass of the magmatic system, as well as systems where crystallisation occurs at greater depth (increased stability of clinopyroxene aids the generation of elevated Ni contents; Hole, 2018). The type of system modelled in the main text may be more analogous to that observed in OIBs with relatively low melt fluxes where ephemeral magma chambers exists for 100s to 1000s of years prior to eruption, and are subject to several periods of recharge. This type of low melt fluxsystem may closely represent regions such as the eastern Galápagos (e.g. Gibson et al., 2016). Nevertheless, magma mixing and recharge may still be an important process that helps to explain some of the considerable spread in the olivine minor element compositions from MORBs.

9. Additional Figures

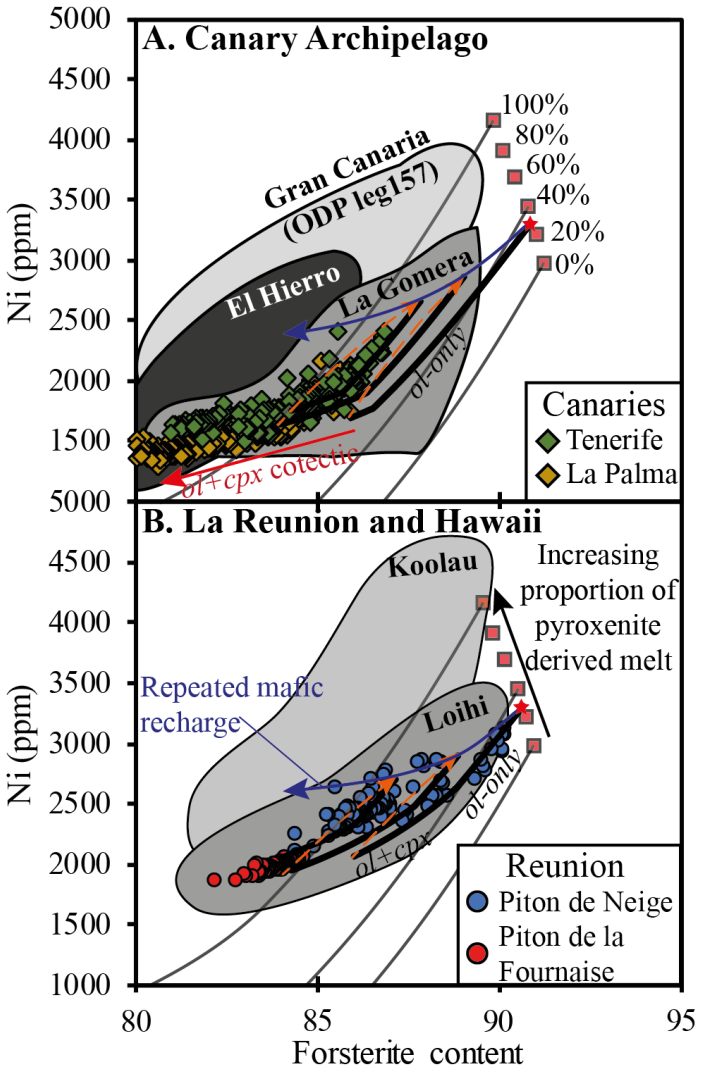

Fig S.5: *Olivine compositions from* ***A.*** *Tenerife and La Palma and* ***B.*** *La Reunion are shown to be consistent with a peridotite source. Tenerife basaltic sample TF2 from Gurenko et al. (2006) was used as a starting composition for fractional crystallization modelling and the initial Ni content was calculated using the method of Matzen et al. (2017a). Due to the higher pressure of melting beneath La Réunion and Tenerife/La Palma the calculated melt Ni content is elevated relative to the low-pressure peridotite-derived melts (fractional crystallisation curves and initial melt solutions (red squares) from Vidito et al. (2013).*

10. Additional references

Chakraborty, S., 2010. Diffusion coefficients in olivine, wadsleyite and ringwoodite. Reviews in mineralogy and geochemistry, 72(1), pp.603-639.

Coogan, L.A. and O'Hara, M.J., 2015. MORB differentiation: In situ crystallization in replenished-tapped magma chambers. Geochimica et Cosmochimica Acta, 158, pp.147-161.

Dasgupta, R., Jackson, M.G. and Lee, C.T.A., 2009. Major element chemistry of ocean island basalts—conditions of mantle melting and heterogeneity of mantle source. Earth and Planetary Science Letters, 289(3-4), pp.377-392.

Geist, D.J., Fornari, D.J., Kurz, M.D., Harpp, K.S., Soule, S.A., Perfit, M.R. and Koleszar, A.M., 2006. Submarine Fernandina: Magmatism at the leading edge of the Galápagos hot spot. Geochemistry, Geophysics, Geosystems, 7(12).

Geist, D.J., White, W.M. and McBirney, A.R., 1988. Plume-asthenosphere mixing beneath the Galapagos archipelago. Nature, 333(6174), p.657.

Gibson, S.A. and Geist, D., 2010. Geochemical and geophysical estimates of lithospheric thickness variation beneath Galápagos. Earth and Planetary Science Letters, 300(3), pp.275-286.

Gibson, S.A., Geist, D.G., Day, J.A. and Dale, C.W., 2012. Short wavelength heterogeneity in the Galápagos plume: Evidence from compositionally diverse basalts on Isla Santiago. Geochemistry, Geophysics, Geosystems, 13(9).

Gibson, S.A., Dale, C.W., Geist, D.J., Day, J.A., Brügmann, G. and Harpp, K.S., 2016. The influence of melt flux and crustal processing on Re–Os isotope systematics of ocean island basalts: Constraints from Galápagos. Earth and Planetary Science Letters, 449, pp.345-359.

Girona, T. and Costa, F., 2013. DIPRA: A user-friendly program to model multi-element diffusion in olivine with applications to timescales of magmatic processes. Geochemistry, Geophysics, Geosystems, 14(2), pp.422-431.

Gurenko, A.A., Hoernle, K.A., Hauff, F., Schmincke, H.U., Han, D., Miura, Y.N. and Kaneoka, I., 2006. Major, trace element and Nd–Sr–Pb–O–He–Ar isotope signatures of shield stage lavas from the central and western Canary Islands: insights into mantle and crustal processes. Chemical Geology, 233(1), pp.75-112.

Harpp, K.S. and White, W.M., 2001. Tracing a mantle plume: Isotopic and trace element variations of Galṕagos seamounts. Geochemistry, Geophysics, Geosystems, 2(6).

Hirose, K. and Kushiro, I., 1993. Partial melting of dry peridotites at high pressures: determination of compositions of melts segregated from peridotite using aggregates of diamond. Earth and Planetary Science Letters, 114(4), pp.477-489.

Hoernle, K., Werner, R., Morgan, J.P., Garbe-Schönberg, D., Bryce, J. and Mrazek, J., 2000. Existence of complex spatial zonation in the Galápagos plume. Geology, 28(5), pp.435-438.

Hole, M.J., 2018. Mineralogical and geochemical evidence for polybaric fractional crystallization of continental flood basalts and implications for identification of peridotite and pyroxenite source lithologies. Earth-Science Reviews.

Lambart, S., Baker, M.B. and Stolper, E.M., 2016. The role of pyroxenite in basalt genesis: Melt-PX, a melting parameterization for mantle pyroxenites between 0.9 and 5 GPa. Journal of Geophysical Research: Solid Earth, 121(8), pp.5708-5735.

Lambart, S., Laporte, D. and Schiano, P., 2009. An experimental study of pyroxenite partial melts at 1 and 1.5 GPa: Implications for the major-element composition of Mid-Ocean Ridge Basalts. Earth and Planetary Science Letters, 288(1-2), pp.335-347.

Lynn, K.J., Shea, T. and Garcia, M.O., 2017. Nickel variability in Hawaiian olivine: Evaluating the relative contributions from mantle and crustal processes. American Mineralogist, 102(3), pp.507-518.

Matzen, A.K., Baker, M.B., Beckett, J.R. and Stolper, E.M., 2013. The temperature and pressure dependence of nickel partitioning between olivine and silicate melt. Journal of Petrology, 54(12), pp.2521-2545.

Matzen, A.K., Baker, M.B., Beckett, J.R., Wood, B.J. and Stolper, E.M., 2017. The effect of liquid composition on the partitioning of Ni between olivine and silicate melt. Contributions to Mineralogy and Petrology, 172(1), p.3.

O'Hara, M.J., 1968. The bearing of phase equilibria studies in synthetic and natural systems on the origin and evolution of basic and ultrabasic rocks. Earth-Science Reviews, 4, pp.69-133.

O'Neill, H.S.C. and Jenner, F.E., 2012. The global pattern of trace-element distributions in ocean floor basalts. Nature, 491(7426), p.698.

Shea, T., Costa, F., Krimer, D. and Hammer, J.E., 2015. Accuracy of timescales retrieved from diffusion modeling in olivine: A 3D perspective. American Mineralogist, 100(10), pp.2026-2042.

Shorttle, O. and Maclennan, J., 2011. Compositional trends of Icelandic basalts: Implications for short–length scale lithological heterogeneity in mantle plumes. Geochemistry, Geophysics, Geosystems, 12(11).

Shorttle, O., Maclennan, J. and Lambart, S., 2014. Quantifying lithological variability in the mantle. Earth and Planetary Science Letters, 395, pp.24-40.

Sobolev, A.V., Hofmann, A.W., Kuzmin, D.V., Yaxley, G.M., Arndt, N.T., Chung, S.L., Danyushevsky, L.V., Elliott, T., Frey, F.A., Garcia, M.O. and Gurenko, A.A., 2007. The amount of recycled crust in sources of mantle-derived melts. Science, 316(5823), pp.412-417.

Thomson, A. and Maclennan, J., 2013. The distribution of olivine compositions in Icelandic basalts and picrites. Journal of Petrology, 54(4), pp.745-768.

Vidito, C., Herzberg, C., Gazel, E., Geist, D. and Harpp, K., 2013. Lithological structure of the Galápagos Plume. Geochemistry, Geophysics, Geosystems, 14(10), pp.4214-4240.

Villagómez, D.R., Toomey, D.R., Geist, D.J., Hooft, E.E. and Solomon, S.C., 2014. Mantle flow and multistage melting beneath the Galápagos hotspot revealed by seismic imaging. Nature Geoscience, 7(2), p.151.

White, W.M., McBirney, A.R. and Duncan, R.A., 1993. Petrology and geochemistry of

the Galápagos Islands: Portrait of a pathological mantle plume. Journal of Geophysical Research: Solid Earth, 98(B11), pp.19533-19563.

Supplementary Data Tables

2019111_Item DR2.xlsx